ISSN: 2754-4915

Journal of Material Sciences & Manufacturing Research

SCIENTIFIC Research and Community

Research Article

Open Access

Biosorption Of 4,4-Ddt from Aqueous Solution Using Moringa Oleifera Pods

Mokete John Phele[1,2*], Fanyana Moses Mtunzi[1,2], Joe Modise[1] and Ikechukwu P Ejidike[3]

[1]Department of Chemistry, Faculty of Applied and Computer Sciences, Vaal University of Technology, Vanderbijlpark, 1911, South Africa

[2]Institute of Chemical and Biotechnology, Faculty of Applied and Computer Sciences, Vaal University of Technology Southern Gauteng Science and Technology Park, Sebokeng, 1983, South Africa

[3]Department of Chemical Sciences, Faculty of Natural, Applied and Health Sciences, Anchor University, Lagos, Nigeria

ABSTRACT

The effectiveness of chemical and thermal pre-treatments on moringa oleifera pod was employed in this investigation as a potent bio-sorbent for Dichlorodiphenyltrichloroethane (DDT) for removal from aqueous solution. The surface chemistry of the Moringa Oliefera pod was characterized using pH at point of zero charge, scanning electron microscopy (SEM), Thermogravimetric analysis (TGA) and Fourier transform infrared spectroscopy (FTIR). The adsorption experiments were conducted in batch at 25, 30 and 45 ^{0}C, both kinetics and equilibrium adsorption tests were performed. Pesticide removal was pH-dependent and found to be maximum at pH 3.5. Adsorption kinetics confirmed that 4,4-DDT adsorption follows a pseudo second - order adsorption kinetic model. The thermodynamic study allows concluding the spontaneous and endothermic character of the adsorption process.

***Corresponding author**

Mokete John Phele, Department of Chemistry, Faculty of Applied and Computer Sciences, Vaal University of Technology, Vanderbijlpark, 1911, South Africa.

Received: June 19, 2025; **Accepted:** June 21, 2025; **Published:** June 28, 2025

Keywords: Adsorption Isotherms, Pesticides, Moringa Oleifera Pods, Kinetics, 4,4-DDT

Introduction

Water quality is currently harmed by the presence of hazardous chemicals, pathogens and radioactive waste in many developing countries. The primary recipients of pollutants released either directly or indirectly from a diverse natural and man-made sources, such as industrial and municipal effluent, and will then be discharged to rivers and lakes [1,2]. Given the possible health risks posed by several contaminants, their pollution poses a hazard to human health [3,4]. Among these pollutants, pesticides are used globally to control insects that can cause and spread some dangerous diseases as well as parasites in agricultural soils [2]. Persistent organic pollutants (POPs), in¬cluding organochlorine pesticides (OCPs), are of global concern because of their toxicity, re¬sistance to degradation, potential for long-term transport and their tendency to accumulate in fatty tissues (lipophilicity), the latter of which renders them likely to bio-accumulate through the food chain [5]. Organochlorine pesticide such as Dichlorodiphenyltrichloroethane (DDTs) are known to have a bioaccumulative nature because of their high lipophilicity and persistence.

In this regard, finding efficient ways to extract this dangerous substance from water is essential. Many studies dealings with the removal of pesticides from water have been reported and relatively few works have reported on the removal of high concentrations of pesticides from water [6]. Several methods are available for pesticide removal such as solid-phase extraction, photocatalysis, photo-fenton, flocculation, ion-exchange, chlorination and ozonisation and adsorption [7-13].

Compared with the different available technologies for the removal of pesticides, adsorption is the most analysed due to its flexibility, simplicity, low cost, and ease of use [14-16]. In addition, it is known for its low consumption of energy and relatively high adsorption capacity [17]. This study aims to investigate the potential of this low-cost biosorbent, M. oleifera pods (MOP) for the removal of 4,4-DDT from aqueous solution. Parameters such as pH, adsorbent dose, and adsorbate concentration that might influence the adsorption efficiency were investigated.

Experimental

Material and Methods

All reagents were of analytical and HPLC grade (Merck, South Africa). Anhydrous sodium sulphate, 99.5% pure, was deactivated by drying in the muffle furnace at 400 °C for 3 h before use. All solvents were subjected to distillation three times before use and were in a range of 99.0 to 99.5% pure. OCP standards were obtained from Department of Water and Sanitation (DWS) research laboratory in Pretoria, South Africa. Kieselgel Merck Type 77754, 70 to 230 mesh 100 µm was purchased from Sigma-Aldrich, South Africa.

Collection and Preparation of Moringa Oleifera Pods

Moringa oleifera pods (MOP) were collected from trees in Limpopo farm near Polokwane. Shortly after being collected, the pods were thoroughly cleaned with doubly distilled deionized water to get rid of any water-soluble contaminants, and they were then oven-dried for 24 hours at 105°C. The washed and dried material was pulverized (by mortar and pestle) and sieved to different mesh sizes. The sieved material was rewashed thoroughly with doubly distilled deionized water to remove the fine particles and dried

for 4 hours at 105°C. The material was treated with 0.1M nitric acid and methanol for 4 hours to remove inorganic and organic matter from the sorbent surface and dried in an electric furnace. The treated and untreated materials were placed in a desiccator to be used as sorbents.

Batch Contact Adsorption Experiments

The effects of various parameters on 4,4-DDT adsorption by MOP were investigated using batch contact adsorption at 25 °C. These experiments were performed with 100 ml of DDT solution (initial concentration 10-100 mg/L), at different contact times (30-360min), adsorbent dosage (1-12 g/L) and pH values (2 -12). For adsorption equilibrium studies 10 mg adsorbent was placed in a series of conical flasks (150 mL) each one containing 100 mL of different initial DDT concentrations (10-100 mg/L) at pH 3.0. The conical flasks were shaken in a rotary orbital shaker at 150 rpm for 60 min.

The experiments were carried out in replicate (n = 3), and blanks were performed. The amount of DDT adsorbed per gram of adsorbate at equilibrium (q_e), at any time (q_t) and the DDT removal percentage (R) were obtained by the Eqs. (1) – (3), respectively:

$$q_e = \frac{(C_0 - C_e)}{M} V \quad (1)$$

$$q_t = \frac{(C_0 - C_t)}{M} V \quad (2)$$

$$R = \frac{(C_0 - C_e)}{C_0} \times 100 \quad (3)$$

Where C_o is the initial DDT concentration (mg/L), C_e is the equilibrium DDT concentration (mg/L), C_t is the DDT concentration at any time (mg/L), m is the adsorbent amount (g) and V is the volume of DDT solution (L).

Adsorption Kinetic Modelling

The successful adsorption process depends on the kinetic parameters. By understanding the adsorption kinetics, the process may be designed and carried out more effectively. Several kinetic models are used to investigate the processes controlling biosorption of adsorbate as well as the rate of mass transfer. Pseudo-first order (PFO) and pseudo second order (PSO) were employed to fit the experimental data. The equations for the models in their non-linearized form are given below.

The PFO rate equation (also, known as Lagergren equation) and the PSO kinetic model are represented in Eqs. 7 and 8 [18].

$$\log(q_e - q_t) = \log q_e - \frac{k_1 t}{2.303} \quad (7)$$

$$\frac{t}{q_t} = \frac{1}{k_1 q_{e2}} + \frac{t}{q_e} \quad (8)$$

Where q_e and qt are the sorption capacity at equilibrium and at time t, respectively (mg/g) and k_1 is the rate constant of pseudo-first-order sorption (min-1). k_2 is the pseudo-second-order rate constant (g/mg/min), qe is obtainable by a linear regression analysis of the $t / q_t = f(t)$ function.

Adsorption Thermodynamics

In order to understand the adsorption process, the three main adsorption thermodynamic parameters, standard free energy (ΔG^0), standard enthalpy (ΔH^0), and standard entropy (ΔS^0), were calculated. The thermodynamic equilibrium constant is approximately equal to the Langmuir adsorption constant [19]. The thermodynamic parameters were calculated through the following equations:

$$\Delta G = -RT \ln K_L \quad (4)$$

Where K_L is the equilibrium constant obtained from Langmuir model, T the absolute temperature (K) and the universal gas constant $R=8.314\times10^{-3}$ kJK−1mol^{-1}. The relationship between K and thermodynamic parameters of ΔH and ΔS can be described by the Van't Hoff correlation in the following equation [20,21]:

$$\ln K = \frac{\Delta S}{R} - \frac{\Delta H}{RT}. \quad (5)$$

Results and Discussion

The major functional groups present in the MOP was characterized by infrared analysis. In the Figure 1 are given FTIR spectra of treated moringa oleifera pod before and after 4,4-DDT adsorption.

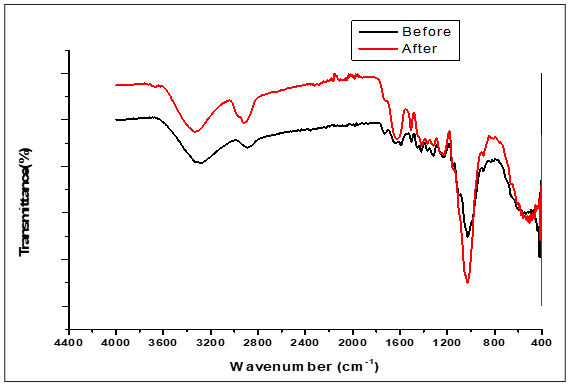

Figure 1: FTIR Spectra of Treated MOP Before and After 4,4-DDT Adsorption

For both FTIR spectrum (Figure 1), peaks were detected in the range of 3200-3500 cm^{-1}; these can be attributed to the presence of hydroxyl groups in proteins, fatty acids, carbohydrates and lignin [22,23]. It is significant to remember that the peak at 3382 cm^{-1} was discovered prior to the adsorption. This displacement occurs due to the hydrogen bond established [24]. The band ranging from 1800 to 1600 indicates the presence of stretches of C = O, which are associated with fatty acids and protein structures. One single peak was found at 1715 for each FT-IR spectrum which also represents stretching vibrations of carboxylic groups [25]. The presence of these components can be noticed once again by the peaks at 1259 and 1264 cm^{-1} [26]. Another peak shift occurred with the 1610 peak to 1587 cm^{-1} after the sorption procedure. This behaviour can be attributed to any modification on the biosorbent surface, since the DDT contains carbonyl groups, secondary and tertiary amines that allow the formation of hydrogen bonds and charge transfer complexes between the components involved [27]. Peaks at 1430 and 1237 cm^{-1} found are assigned to axial deformations of C–N groups in amines and amides.

Scanning Electron Microscopy

Figure 2 displays an image of the MOP at 400 magnification levels. The macro porous structure, fibrous structure, and highly variable morphological feature are all visible. The SEM of the MOP clearly shows that the morphology did not have regular shape and size, and presents porosity.

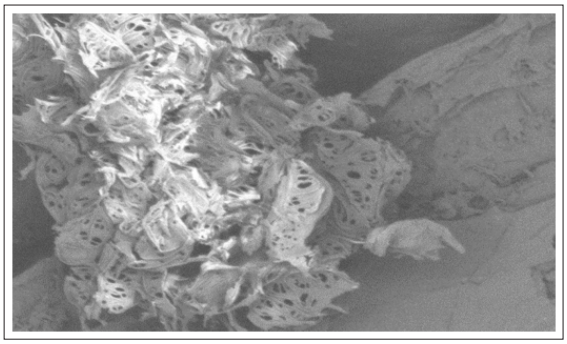

Figure 2: SEM Micrograph of Treated MOP

Mesoporous structures with a range of pore diameters are seen in the MOP micrographs. Because of the bonding voids that are available for DDT, these surface characteristics would lead to high bonding. Around the edges, tiny holes were discovered, suggesting the potential for sorption on a smaller scale. This structure facilitates the processes of ion adsorption, due to the interstices and, more importantly, to the presence of the protein component of the seed. Thus, based on these characteristics, it can be concluded that this material has an adequate morphological profile for retaining 4,4-DDT.

Thermogravimetric Analysis

Thermogravimetric analysis was used to characterize the decomposition stages and thermal stability of the MOP. The mass loss curve for one sample can be observed in Figure 3, showing a typical profile that indicates several stages of the decomposition process. This thermogravimetric curve verifies the sample heterogeneity, since the intermediates formed are a mixture of several components. The mass loss curve can be divided into three stages:

- From 30°C to 124°C mass loss in the order of 8%, associated with water desorption, was observed. The amount of water loss from MOP determined by this technique is similar to the value of 8.9% found by Anwar & Rashid;
- In the second step 32% of mass loss was observed in the temperature range of 124°C to 266°C. This stage occurs due to the decomposition of organic matter, probably the protein components, present in MOP; and
- The third step occurs from 266°C to 540°C with decomposition of the greater part of the seed components, which probably includes fatty acids, for example oleic acid has a boiling point of 360°C. At 950°C a total residue of around 14.6% was observed, due the presence of ash and probably inorganic oxides [28].

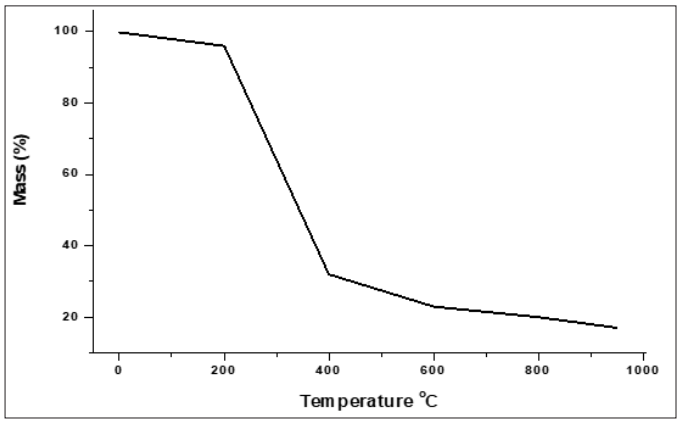

Figure 3: Thermogravimetric Curve for MOP

Zeta Potential Results

Figure 4 shows the plot of the potential zetal against pH (from 2 to 12). The curve behaviour indicates that the biosorbent surface has a primarily negative charge at pH values over 4.5. Additionally, the zero-point charge of the material surface is represented by the isoelectric point, which is 4.5. After a 24-hour sorption process at 25°C, the zeta potential was measured in triplicate using 50 mL of 4,4-DDT solution at pH 3.5 and 10 mg of MOP. Values of -36.09, -36.43, and -38.32 mV were discovered. These numbers suggest that the negative charges on the biosorbent's surface increased. Because the particle has become even more negative, it is therefore possible to confirm that the adsorption of 4,4-DDT is independent of the electrostatic attraction condition. According to He, et al., the adsorption of 4,4-DDT is related to the nature of organic matter involved in the process, which increases the affinity between the contaminant and the biosorbent [29]. This is possible due to the surface area and functional groups (aromatic rings, hydroxyl compounds and carboxylic groups) present in the adsorbent surface, increasing the non-ionic interactions, such as van der Walls and π–π bonds.

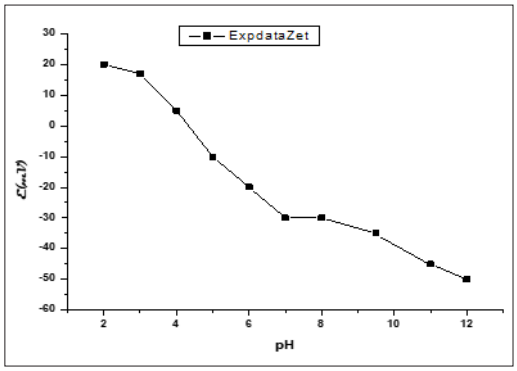

Figure 4: Zeta Potential Curve for MOP.

The Effect of Adsorbent Dose

The data are presented in Figure 5 to show how the pH and dosage affect the 4,4-DDT biosorption capability. It is feasible to observe that when both parameters decrease simultaneously, the adsorption capacity increases by about 3.0 mg/g. A little drop in 4,4-DDT was seen when the pH of the solution was raised from 3 to 9, suggesting that low pH favoured 4,4-DDT sorption when taking into account the adsorption capacity tendency. Furthermore, following the sorption processes, there was little change in the pH of the solutions.

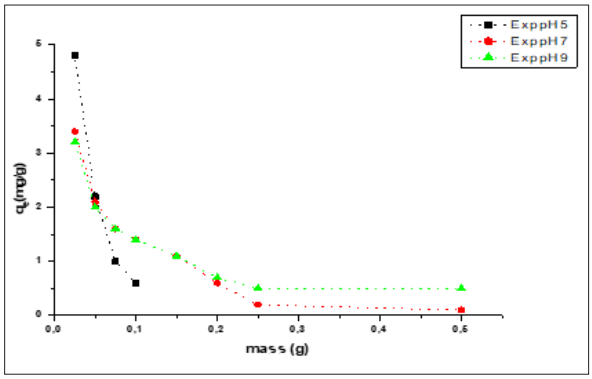

Figure 5: The Effect of the Biosorbent Mass on the Adsorption Capacity (q_e)

The N, H, and O atoms of the 4,4-DDT molecule and groups on the adsorbent's surface create hydrogen bonds, which are common at lower pH values and account for the highest adsorption capacity levels at pH 3.5.

Effect of Adsorbent Particle Size

To analyse the effect of particle size on the adsorption process, studies were carried out on various particle sizes of the adsorbents, ranging from 2 mm to 20 mm, as shown in Figure 6. The findings indicate that the 4,4-DDT adsorption capacity increased from 92 to 97 and the adsorbent size decreased from 2 mm to 20 mm in accordance with mesh size. This indicates that the amount of 4,4-DDT adsorbed increases positively as the mesh size and, consequently, the particle size decrease. This is accurate since smaller particles have a larger surface area when the mesh size decreases. This phenomenon may be explained by the fact that when mesh size lowers, the particle size reduces and the surface area increases. Furthermore, the adsorbents' smaller particles maximize the adsorbate's capacity to penetrate the interior pores of the adsorbent by shortening the diffusion routes [30]. As a result, higher 4,4-DDT adsorption was noted, and for further experimental research, a particle size of 250 mm was chosen.

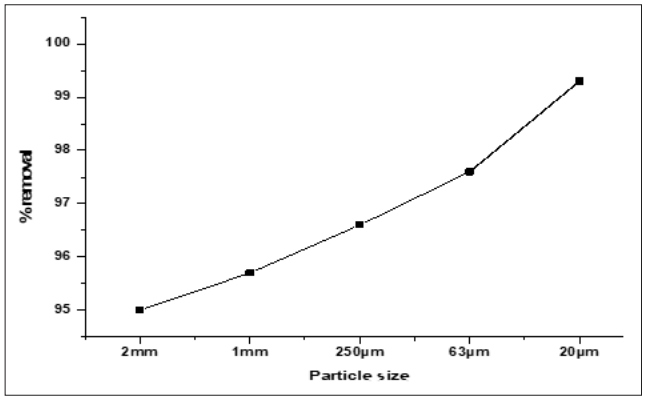

Figure 6: Adsorbent Particle Size Effect on the Adsorption of 4,4-DDT

Effect of Initial Concentration of 4,4-DDT Aqueous Solution

Since a certain quantity of adsorbent may adsorb a specified quantity of pesticide from an aqueous solution, the 4,4-DDT initial concentration is an essential parameter in adsorption research. Figure 7 illustrates the effect of the adsorbate's initial concentration, demonstrating that as the adsorbent's initial concentration increased, its adsorption effectiveness declined. At various initial concentrations of 10, 25, 50, 75 and 100 mg/L, the decrease in the percent removal of pesticide was observed in the range of 95.8–90.08% for 4,4-DDT. Larger active sites at lower sorbate ion/sorbent ratios are implicated in sorbate ion sorption, it can be concluded. Saturation at higher energy points happens in tandem with an increase in sorbate ions relative to sorbent ions, and adsorption begins at lower energy sites, resulting in a decrease in the adsorption percentage [31]. The reduction in the initial concentration of adsorbate Because there were enough surface-active sites, a progressive development in the adsorption of adsorbate on the adsorbent surface was observed.

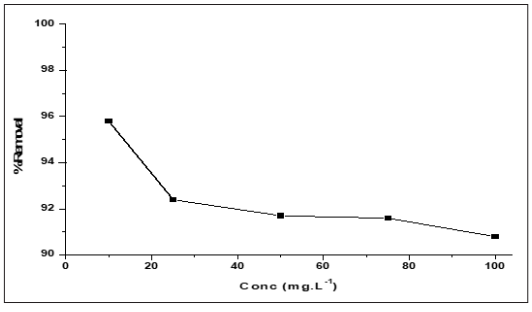

Figure 7: Initial Concentration Effects on the Uptake of 4,4-DDT

Effect of Contact Time

The contact time effect on sorption of 4,4-DDT by MOP was investigated at 10 mg/L adsorbate initial concentration, 100 mg/L mass adsorbent, pH 3. The removal percentage of a mixture of the 4,4-DDT was measured at different contact times (30, 60,120, 240, and 360 min). The pesticide uptake rate on the adsorbent (MOP) is evident from Figure 8, It demonstrates that as contact time increases, pesticide sorption increases favourably. Initially adsorption showed a quite rapid pattern, followed by a gradual slowdown before achieving a final equilibrium position. An increase in the percentage of adsorption was recorded from 72.9 - 79.3% on MOP. Initially pesticide uptake by the sorbent was too quick because of the presence of abundant vacant positions for sorption, but as the contact time prolongs from 120 minutes, the adsorption rate was reduced.

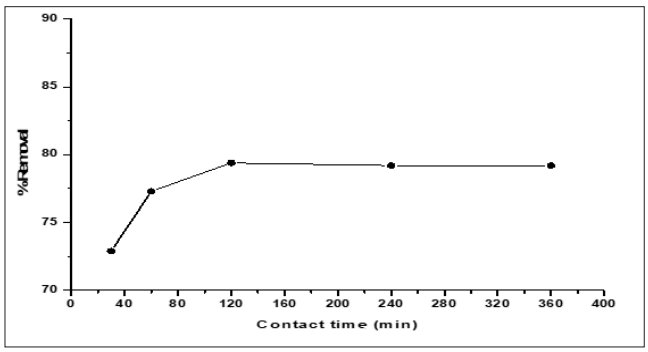

Figure 8: The Effect of Contact Time on the Uptake of Pesticides

Adsorption Kinetics

Figure 9 & 10 represents the adsorption kinetic curves of 4,4-DDT at different temperatures (25, 30 & 45°C), adsorption was slow for 4,4-DDT, requiring around 200 min to achieve equilibrium.

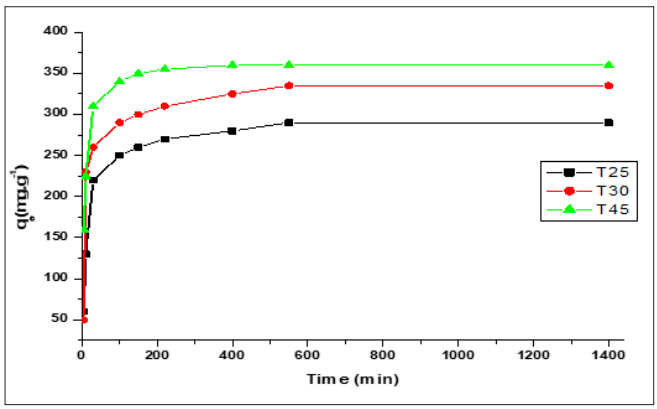

Figure 9: Kinetic Curves of Adsorption of 4,4-DDT on the MOP at 25, 30, and 45 °C. (1st Order)

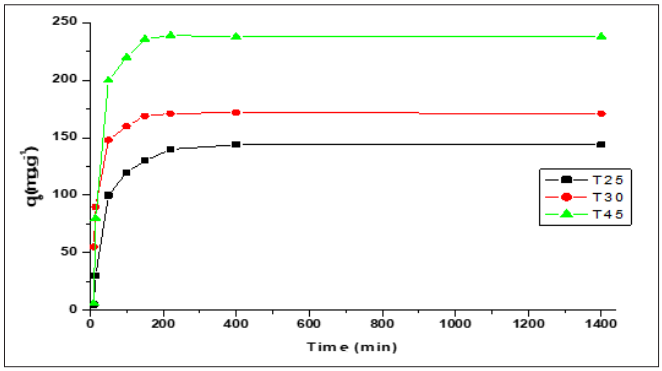

Figure 10: Kinetic Curves of Adsorption of 4,4-DDT on the MOP at 25, 30 & 45 °C. (2nd Order)

Many models were used in the literature to determine the kinetic parameters, comprehend the adsorption mechanisms, and identify the rate-limiting step [32]. Two models were examined in the current investigation, specifically pseudo-first order and pseudo-second order. The regression coefficients and associated parameters derived from fitting the models to the experimental adsorption kinetic data are summarized in Table 1 along with the non-linear version of each equation.

Table 1: Adsorption Isotherms Modelling for the 4,4-DDT

Models	Non-Linear Expression	Values of the Parameters	R^2
1st Order	$q_e=q_e(1-e^{-tk1})$	T = 25 ◦C; qe = 271.4 mg/g; k_1 = 0.073	0.969
		T = 30 ◦C; qe = 310.9 mg/g; k_1 = 0.095	0.979
		T = 45 ◦C; qe = 340.7 mg/g; k_1 = 0.097	0.980
2nd Order	$q_t = \frac{k_2 q_e^2 t}{1 + k_2 q_e t}$	T = 25 ◦C; qe = 290.9 mg/g; k_2 = 0.00052	0.984
		T = 30 ◦C; qe = 330.0 mg/g; k_2 = 0.00056	0.987
		T = 45 ◦C; qe = 367.3 mg/g; k_2 = 0.00065	0.992

The pseudo second-order model provided the greatest fitting for 4,4-DDT adsorption on the MOP, based on the results.

Thermodynamics

The values of the thermodynamic parameters found for the adsorption of 4,4-DDT pesticide are compiled in Table 2. As is typical in adsorption, spontaneous processes are characterized by negative values of the standard free energy for the adsorbate.

Table 2: Thermodynamic Parameters of the 4,4-DDT Pesticide Adsorption.

Pollutant	T (◦C)	ΔG^0 (kJ·mol^{-1})	ΔH0 (kJ·mol^{-1})	ΔS0 (kJ·mol^{-1}·K^{-1})
DDT	25	-26.6	16.91	0.145
	30	-29.3		
	45	-32.4		

The standard enthalpy for 4,4-DDT adsorption is 16.91 kJ.mol^{-1}. The comparatively low value is typical with mostly physical adsorption, whereas the positive value suggests that the adsorption process of this molecule is endothermic. Entropy is typically -0.146 kJ.mol-1K^{-1}. Though it should be noted that the value is extremely low, it does, in fact, imply no appreciable change in entropy during adsorption. The negative value indicates a decrease in the randomness of the molecules at the solid-liquid interface and a higher ordering of the 4,4-DDT molecules after they have been adsorbed on the activated carbon surface.

Conclusion

Kinetics and equilibrium isotherms of the non-competitive adsorption of pesticides, such as 4,4-DDT, onto moringa oliefera pod from the aqueous solution have been investigated. Samples of activated carbon were made under particular circumstances in order to assess how different adsorbent qualities affected the adsorption of the pesticide under study and the moringa's performance. Since 10 mg of treated moringa was able to remove more than 79% of 4,4-DDT from 50 ml of pesticide solution, the study provided insight into the use of processed moringa as an inexpensive adsorbent for pesticide removal from aqueous solutions. In contrast to the pseudo-first-order model, the results of various kinetic models that were used to fit the experimental data better described the pseudo-second order model for the adsorption of 4,4-DDT on treated moringa oleifera pod. These findings show that moringa oleifera pod, which is widely accessible, may be a useful and reasonably low-cost adsorbent for removing pesticide from aqueous solution.

Acknowledgements

The authors thank the Department of Chemistry Vaal University of Technology, Vanderbiljpark, South Africa for funding this work and the support.

Conflict of Interest

The authors declare that there is no conflict of interests regarding the publication of this article.

References

1. Rajeshkumar S, Mini J, Munuswamy N (2013) Effects of Heavy Metals on Antioxidants and Expression of HSP70 in Different Tissues of Milk Fish (Chanos chanos) of Kaattuppalli Island, Chennai, India. Ecotoxicol Environ Saf 98: 8-18.
2. Harabawy ASA, Ibrahim ATA (2014) Sublethal Toxicity of Carbofuran Pesticide on the African Catfish Clarias Gariepinus (Burchell, 1822): Hematological, Biochemical and Cytogenetic Response. Ecotoxicol Environ Saf 103: 61-67.
3. Binh QA, Nguyen HH (2020) Investigation the Isotherm and Kinetics of Adsorption Mechanism of Herbicide 2,4-Dichlorophenoxyacetic Acid (2,4-D) on Corn Cob Biochar. Bioresour Technol Rep 11: 100520.
4. Salman JM, Hameed BH (2010) Adsorption of 2,4-Dichlorophenoxyacetic Acid and Carbofuran Pesticides onto Granular Activated Carbon. Desalination 256: 129-135.
5. Jones KC, De Voogt P (1999) Persistent organic pollutants: State of the science. Environ Poll 100: 209-221.
6. Bandala ER, Octaviano JA, Pastrana P, Torres LG (2006) Removal of aldrin, dieldrin, heptachlor, and heptachlor epoxide and/or pseudomonas fluorescens free cell cultures. Journal of Environmental Science and Health, Part B 4: 553-569.
7. Souza DA, Lancas FM (2003) Solventless sample preparation for pesticides analysis in environmental water samples using solid-phase microextration-high resolution gas chromatography/mass spectrometry. Journal of Environmental Science and Health, Part B 38: 417-428.
8. Franco-Garcia ML, Murat M, Percherancier JP, Pouyet B (1996) Investigation of aqueous adsorption desorption of

pesticide on SiO2. Fresenius Environmental Bulletin 5: 563-568.

9. Fallmann H, Krutzler T, Bauer R, Malato S, Blanco J (1999) Applicability of the Photo- Fenton method for treating water containing pesticides. Catalysis Today 54: 309-319.
10. Thebault P, Cases JM, Fiessinger F (1981) Mechanism underlying the removal of organic micro pollutants during flocculation by an aluminium or iron salt. Water Research 15: 183-189.
11. Varhney KG, Khan AA, Gupta U, Maheswari SM (1996) Kinetics of adsorption on antimony (v) phosphate cation exchanger: evaluation of the order of reaction and some physical parameters. Colloids and Surfaces, A: Physicochemical and Engineering Aspects 113: 19-23.
12. Mason YZ, Choshen E, Rav-Acha C (1990) Carbamate insecticides: Removal from water by chlorination and ozonation. Water Research 24: 11-21.
13. Ahmad T, Rafatullah M, Ghazali A, Sulaiman O, Hashim R, et al. (2010) Removal of pesticides from water and wastewater by different adsorbents: a review. J Environ Sci Health Part C 28: 231-271.
14. Fiorenza R, Di Mauro A, Cantarella M, Privitera V, Impellizzeri G (2019) Selective Photodegradation of 2,4-D Pesticide from Water by Molecularly Imprinted TiO2. J Photochem Photobiol A: Chem 380: 111872.
15. Sellaoui L, Yazidi A, Taamalli S, Bonilla-Petriciolet A, Louis F, et al. (2021) Adsorption of 3-Aminophenol and Resorcinol on Avocado Seed Activated Carbon: Mathematical Modelling, Thermodynamic Study and Description of Adsorbent Performance. J Mol Liq 342: 116952.
16. Zhang Z, Wang T, Zhang H, Liu Y, Xing B (2021) Adsorption of Pb (II) and Cd (II) by Magnetic Activated Carbon and Its Mechanism. Sci Total Environ 757: 143910.
17. Zhu J, Li Y, Xu L, Liu Z (2018) Removal of Toluene from Waste Gas by Adsorption-Desorption Process Using Corncob-Based Activated Carbons as Adsorbents. Ecotoxicol Environ Saf 165: 115-125.
18. Ho YS, McKay G (1998) Sorption of dye from aqueous solution by Peat. Chem Eng J 70: 15-124.
19. Liu Y (2009) Is the free energy change of adsorption correctly calculated?. Chem Eng J 54: 1981-1985.
20. Celik MS, Ozdemir O (2018) Heterocoagulation of hydrophobized particulates by ionic surfactants, Physicochem. Probl Miner Process 54: 124-130.
21. Yildiz N, Erol M, Aktas Z, Alimli AC (2004) Adsorption of aromatic hydrocarbons on BTEA-betonites. Adsorpt Sci Technol 22: 145-154.
22. Baptista ATA, Silva MO, Gomes RG, Bergamasco R, Vieira MF, et al. (2017) Protein fractionation of seeds of Moringa oleifera lam and its application in superficial water treatment. Sep Purif Technol 180: 114-124.
23. Fagbohun A, Adebiyi A, Adedirin O, Fatokun A, Afolayan M, et al. (2014) Instrumental and chemical characterization of Moringa oleifera Lam root starch as an industrial biomaterial. Res Pharm Biotechnol 3: 7-12.
24. Nada AMA, Shabaka AA, Yousef MA, Abd-El-Nour KN (1990) Infrared spectroscopic and dielectric studies of swollen cellulose. J Appl Polym Sci 40: 731-739.
25. Neto VOS, Oliveira AG, Teixeira RNP, Silva MAA, Freire PTC, et al. (2011) Use of coconut bagasse as alternative adsorbent for separation of copper (II) ions from aqueous solutions: isotherms, kinetics, and thermodynamic studies. Bio Resources 6: 3376- 3395.
26. Sanches NB, Pedro R, Diniz MF, Mattos EC, Cassu SN, et al. (2013) Infrared spectroscopy applied to materials used as thermal insulation and coatings. J Aerosp Technol Manag 5: 421-430.
27. Senesi N, Testini C (1983) Spectroscopic investigation of electron donor-acceptor processes involving organic free radicals in the adsorption of substituted urea herbicides by humic acidsa. Pestic Sci 14: 79-89.
28. Anwar F, Rashid U (2007) Physico-chemical characteristics of Moringa oleifera seeds and seeds oil from a wild provenance of Pakistan. J Bot 39: 1443-1453.
29. He XS, Zhang YL, Liu ZH, Wei D, Liang G, et al. (2020) Interaction and coexistence characteristics of dissolved organic matter with toxic metals and pesticides in shallow groundwater. Environmental Pollution 258: 113736.
30. Gupta VK, Ali I (2001) Removal of DDD and DDE from wastewater using bagasse fly ash, a sugar industry waste. Water Research 35: 33-40.
31. Okoya AA, Adegbaju OS, Akinola OE, Akinyele AB, Amuda OS (2020) Comparative assessment of the efficiency of rice husk biochar and conventional water treatment method to remove chlorpyrifos from pesticide polluted water. Current Journal of Applied Science and Technology 39: 1-11.
32. Aksu Z, Kabasakal E (2004) Batch Adsorption of 2,4-Dichlorophenoxy-Acetic Acid from Aqueous Solution by Granular Activated Carbon. Sep Purif Technol 35: 223-240.